Orbitronics - Harnessing Metal Insulator Phase Transition in 1T-$MoSe_2$

Ram Krishna Ghosh
Department of Electrical Engineering,
University of Notre Dame,
Notre Dame, IN 46556, USA

Suman Datta
Department of Electrical Engineering,
University of Notre Dame,
Notre Dame, IN 46556, USA

***Abstract*— In this work, we reveal a remarkable orbital ordering texture associated with a Peierls distortion that leads to metal-insulator phase transition (MIT) in 1T molybdenum diselenide ($MoSe_2$). The metallic conductivity in this MIT is realized by an isotropically distributed Mo t_{2g} orbitals whereas splitting of both t_{2g} and e_g orbitals near the Fermi level opens a bandgap in distorted semiconducting phase. Our results also indicate that a stacking of two orbitally ordered layers allows triggering of phase transition by external perturbations such as, vertical pressure and vertical electric field.**

Keywords*— Peierls distortion; charge density wave; metal-insulator phase transition; density functional theory.

I. Introduction

In current research, most of the development on devices are limited on the 2H (trigonal prismatic) form of transition metal dichalcogenide (TMD) structure, which shows indirect to direct bandgap transition when the dimensionality goes down to their monolayer limit [1-3]. However, 1T (octahedral) phases are still remain largely unexplored. Interestingly, the partial filling of '*d*' orbitals in these 1T layered compounds show fascinating behavior of structural evolution and attract enormous attention for exceptional electronic properties. Especially, Peierls distortion associated with charge density wave (CDW) instability is one of a remarkable and surprising feature of these 1T materials [4-5]. Recent observations on different 1T phases indicate an occurrence of phonon softening by Fermi-surface driven instability which spontaneously breaks the lattice symmetry of the crystal. As a consequence, these crystals show a periodic modulation in charge densities by forming distinct CDWs. When this CDW is imprinted on a lattice, a new orbital ordering is also prompted and that eventually leads to unusual electronic behavior like superconductivity or Metal insulator transition (MIT) in these materials [4]. Even though the origin of CDW scenario is quite well known for TaS_2, $TaSe_2$, and $TiSe_2$, [4-6] there is still a lack of understanding in various CDW induced structural phase transition in group IV dichalcogenides and their contribution in transport properties. In this work, we explore a metal insulator phase transition by the orbital ordering associated with CDW in 1T-$MoSe_2$. We also demonstrate a reversible IMT in a stacking of two orbitally ordered layers by two external stimuli and show an abrupt switching characteristics with a conductance change over eight decades. This not only gives insight into the fundamental properties of opening and closing of the bandgap in this 2D material, but also marks an important milestone towards the realization of ultra-low power device applications for 2D materials beyond conventional MOSFETs.

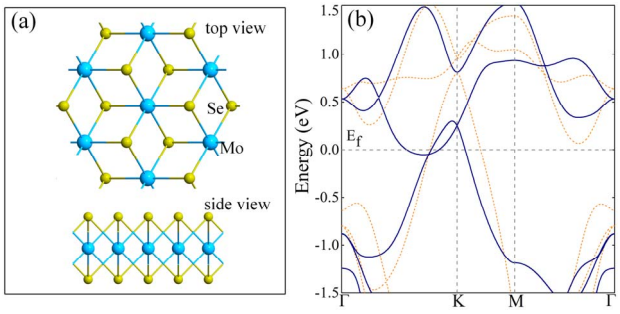

Fig. 1. (a) Atomic configuration in undistorted 1T $MoSe_2$ phase and (b) The electronic band structure of both bulk (blue line) and monolayer form (dotted orange line).

II. Computational Details

The simulations are performed using *ab-initio* density functional theory (DFT) as implemented in the Atomistic-ToolKit [7]. We use Broyden-Fletcher-Goldfarb-Shannon (BFGS) scheme to optimize different crystallographic forms of 1T-$MoSe_2$ until all the forces acting on atoms become smaller than 0.001 eV/Å and the stress is less than 0.0001 eV/Å^3. We also use non-equilibrium Green's function (NEGF) based transport calculations in the ballistic limit to calculate the conductance.

III. Results and Discussions

To describe the detail of the structural and electronic properties corresponding to the CDW phases, we first investigate the properties of undistorted 1T-$MoSe_2$ (p-3m1), as shown in Fig. 1(a). The band structures in Fig. 1(b) clearly indicate that, the 1T-$MoSe_2$ is semi-metallic in nature. In monolayer, both the 'electron' and 'hole-like' bands crossing the Fermi level (E_f) give rise to both electron and hole pockets in the Fermi surface whereas only 'hole-like' bands form hole pockets in the bulk crystal. In agreement with earlier report [8], we find that these 'hole-like' bands are primarily composed of 4-d_{xy} orbitals centered on Mo atoms that mainly contribute to the electron densities of these metallic bands (see later). This

978-1-5090-0818-6/16/$31.00 ©2016 IEEE

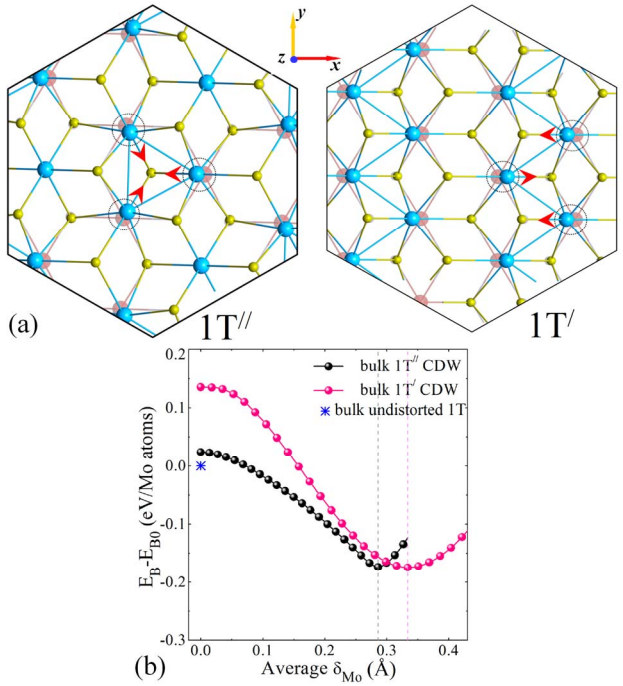

Fig. 2. (a) Atomic conformations of $MoSe_2$ CDW phases where the shaded atoms indicate their original undistorted positions. The Mo displacements as indicated by red arrows are in the *xy* plane. Alternative Mo atoms exhibit trimerization in 1T″ whereas chain-like dimer formation occurs in between of Mo atoms in 1T′. (b) The relative change in binding energy as a function of average displacement of the Mo atoms. E_B and E_{B0} are the binding energies of the distorted and undistorted phases of 1T $MoSe_2$, respectively.

pristine form is a metastable phase associated with in-plane soften phonon modes of Mo atoms and indicates a possibility of structural transition to a commensurate CDW phase driven by a strong electron-phonon coupling within the crystal.

To illustrate the CDW phases in our *ab-initio* calculations, we choose two real-space supercells with $2a_0 \times 2a_0$ and $2a_0 \times a_0$, (referred as 1T″ and 1T′, respectively) to verify the displacements of the atoms from their original positions. Interestingly, atomic relaxation of these supercells gives different shifting of Mo atoms from their primitive positions and forms two new Peierls distortion in this TMD as shown in Fig. 2(a). In the 1T″ CDW phase, three Mo atoms alternatively come closer to each other (indicated by red arrow) and form an in-plane trimer like clustering in the crystal whereas in 1T′, one Mo atom moves opposite to the other two Mo atoms and forms a dimer like pattern. These formations show a significant lowering in binding energy ($E_B = E_{total} - n_{Mo}E_{Mo} - n_{Se}E_{Se}$) [9] which points a stabilization of the CDW phases over the undistorted one. This CDW phase can also drastically change the electronic properties of the material. In 1T″, the material is able to open a direct energy band gap at the high symmetry point '*K*' (see Fig. 3 for monolayer) from bulk to monolayer limit. This indeed implies a metal-insulator transition associated with the emergence of commensurate CDW phase within the crystal. On the contrary, monolayer 1T′ also undergoes a MIT similar to 1T″. However, the bulk 1T′ remains semi-metal with a different band structure profile. Fig. 3(b) shows the bandgap of monolayer 1T″ by using three diffe-

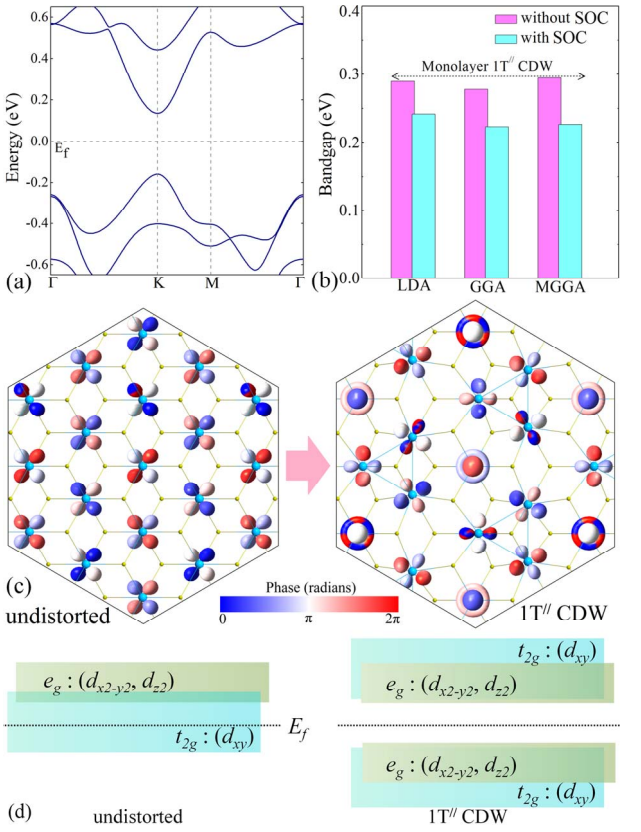

Fig. 3. (a) The LDA band structure of monolayer 1T″ CDW phase and (b) the bandgap values. SOC = spin-orbit coupling. (c) Top view of the orbital texture of the highest occupied molecular orbitals (HOMO) in the undistorted and 1T″ phases and (d) a schematic showing orbital ligand splitting.

rent DFT functionals, such as, local density approximation (LDA) and generalized gradient approximation (GGA) and meta-GGA (MGGA). Generally, LDA and GGA have a tendency to underestimate the energy bandgap compared to the meta-GGA [10]. Interestingly, here we find that the bandgap value obtained by MGGA is nearly same as the LDA one. Besides, the spin-orbit coupling (SOC) also has a significant effect on the band structure of both bulk and monolayer 1T″. The conduction band minima (CBM) and the valence band maxima (VBM) of 1T″ $MoSe_2$ split under SOC and consequently the bandgap also reduces (Fig. 3(b)) by keeping the overall band profile same. In contrast, the SOC does not have any substantial influence on the 1T′ band structure. To investigate the chemical origin of this dramatic change in the electronic properties of CDW phases, we calculate the charge density distribution of the highest occupied molecular states (HOMO) in real space to compare with the undistorted case. In Fig. 3(c), the charge densities in undistorted phase originate from t_{2g} orbitals of an equally distributed Mo 4-d_{xy} orbitals. Whereas, a dispersed e_g orbitals remain in high energy states which couples with the t_{2g} orbitals to conserve the charge in this crystal. However, a complex orbital texture emerges in the crystal when it forms 1T″. Mainly, the in-plane '*d*' orbitals (i.e. d_{xy} and d_{x2-y2}) from Mo atoms forming the trimers and out-of-plane d_{z2} orbitals from other Mo atoms contribute to these charge densities. Interestingly, Se atoms do not participate in

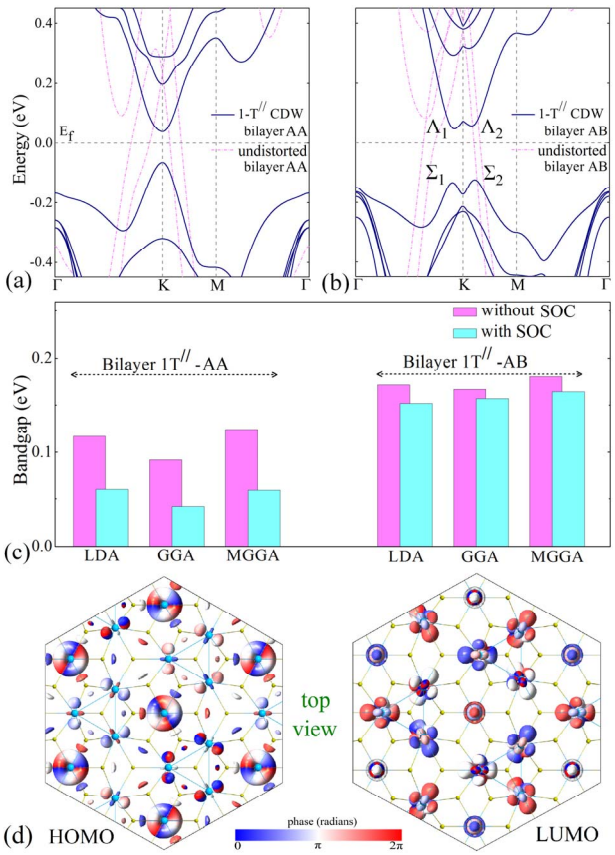

Fig. 4. (a)-(b) The LDA band structure of bilayer undistorted (pink dotted line) and 1T″ phases (blue solid line) in AA and AB stacked configurations. (c) The corresponding bandgap values for different functionals used in DFT calculations where SOC indicates the inclusion of spin-orbit coupling. (d) Top view of the orbital texture of HOMO and LUMO at the 'K' of the Brillouin zone of the relaxed 1T″ AA stacking.

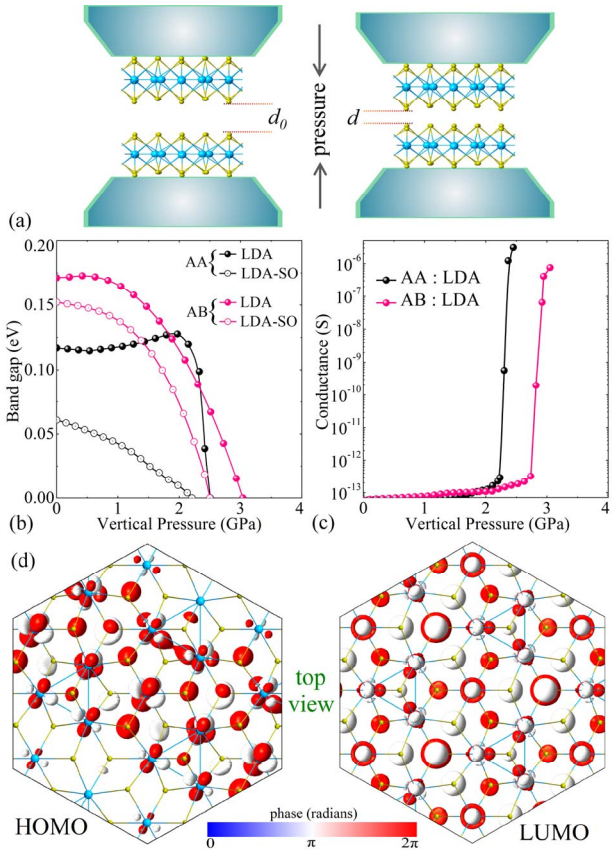

Fig. 5. (a) Schematic of the atomic structure of AA configuration under vertical pressure. (b)-(c) The variation of bandgap and conductance of 1T″ AA and AB stacking under the applied vertical pressure. (d) Top view of HOMO at the 'Γ' valley and LUMO near the 'K' of the Brillouin zone of the metallic 1T″ AA stacking under an applied vertical pressure of 2.50 GPa.

this orbital texture of 1T″. That means the in-plane states form *d-d* overlaps in between trimer atoms which eventually couple with other t_{2g} orbitals situated on the non-trimer Mo atoms. This similar ligand splitting can also be observed in lowest unoccupied molecular states (LUMO). This implies that the formation of trimerization not only makes a downshift of e_g but also leads to a splitting of both t_{2g} and e_g bands to open a bandgap in the 1T″ CDW phase as schematically shown in Fig. 3(d). On the other hand, a reduced bond length of Mo-Se arises along the zigzag formations in 1T′ phase which eventually increases the *p-d* overlap of the orbitals. Therefore, a hybridized Mo-d_{xy} and Se-p_x orbital along the zigzag Mo line contributes to the orbital distributions which depopulates the t_{2g} orbitals and opens a bandgap in monolayer 1T′. Therefore, this metal insulator transition is intertwined with a complex orbital texture associated with strong electron-phonon coupling in this CDW phase, which is the key result of this analysis. Fig. 4 presents the band structure properties of bilayer structures of 1T″ in both AA and AB stacking order. Similar to the monolayer 1T″, the AA stacking has direct bandgap at 'K' (see Fig. 4(a)) whereas the band structure of AB stacking shows an indirect bandgap in between 'Λ_1' and 'Σ_2' as depicted in Fig. 4(b). The interlayer interactions and a slight increase in lattice parameters in bilayer 1T″ reduce the bandgap quite significantly. To gain the insight, we further examine the orbital textures of both highest occupied and lowest unoccupied (HOMO and LUMO) as shown in Fig. 4(d). The contribution comes mostly from the Mo sites rather than the Se sites. Interestingly, within the HOMO charge distribution, the in-plane d_{xy} and d_{x2-y2} orbitals on trimer Mo sites are less localized than the out-of-plane d_{z2} orbitals coming from non-trimer Mo atoms. However, a completely opposite scenario can be seen in the LUMO texture where d_{xy} and d_{x2-y2} orbitals on trimer Mo sites mostly contribute to the charge distribution. We notice a similar nature of charge localization in AB stacking of 1T″ bilayer systems. Therefore, these new orderings of confined and localized charges in this CDW phase play a crucial role in the opening of the band gap in 1T″ bilayer which is absent in undistorted 1T bilayer structure. On the other hand, interlayer interactions arising from Se-*p* orbitals in bilayer 1T′ structures makes them semi-metallic in character similar to the bulk case. Therefore, a dimensionality driven metal insulator phase transition can also be seen in 1T′ CDW phase.

As we can see that the electronic properties of CDW phases are greatly influenced by relative orbital ordering, therefore, one can expect a possibility to modulate the electronic properties by controlling the orbital ordering by external pertu-

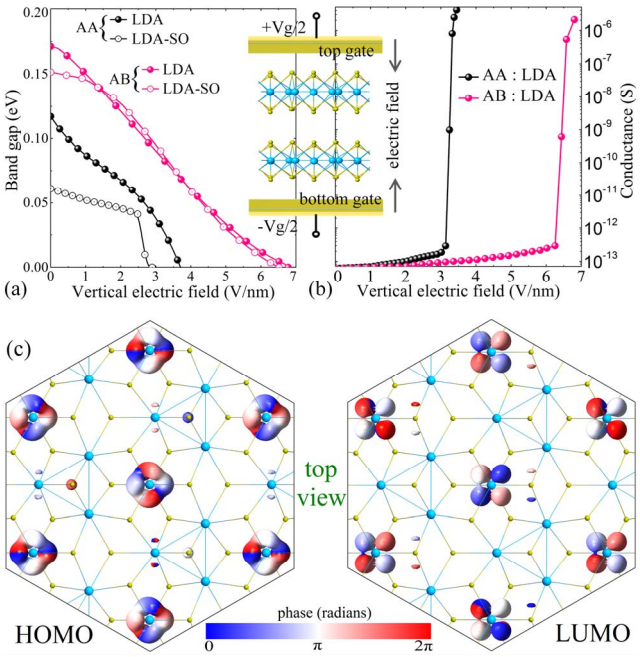

Fig. 6. (a)-(b) The variation of bandgap and conductance under the applied vertical electric field (inset) (c) Top view of HOMO at the 'K' valley and LUMO near the 'K' of the Brillouin zone of the 1T″ AA stacking under an applied electric field of 3.75 V/nm.

rbations. So, here we explore the effect of vertical pressure and vertical electric field on the electronic phase transition in semiconducting bilayer 1T″. In this section, we explore the electronic properties by LDA functional only as the LDA bandgaps are quite close to MGGA and it efficiently describes the band structure evolution under external perturbations. Fig. 5(a) shows the schematic of the bilayer 1T″ phase under vertical pressure. Under the influence of vertical pressure the interlayer distance reduces which increases the interlayer coupling and redistributes the localized charges to alter the electronic nature of the material. Specially, the bandgap decreases (Fig. 5(b)) and after a critical pressure the bands crosses the Fermi level and makes a reversible insulator metal transition (IMT) in this material. Interestingly, with the SOC consideration, the splitting at the band extrema increases with pressure and make the IMT at a faster rate. As illustrated in Fig. 5(d), we can immediately observe a change in the orbital texture where the Se *p*-orbitals start contributing to the charge ordering in comparison to the relaxed condition (Fig. 4(d)). Besides, the highly localized d_{z2} charge densities also spread out from their positions whereas the trimer Mo atoms gain further charge accumulation. Likewise, the localized charges in LUMO also spread out and form a new orbital texture in this material. A similar phenomenon of orbital reordering occurs in AB stacking where the bandgap gradually decreases to zero to induce an IMT. Our non-equilibrium Green's function (NEGF) based transport calculations indicate a very sharp conductance change of eight orders of magnitude across the IMT (Fig. 5(c)) in the ballistic limit. In the same way, a reversible IMT with a conductance change of ~10^8 can also be realized under vertical electric field (Fig. 6) with a new orbital texture (see Fig. 6(c)) across the transition. Therefore, one can control and obtain a very abrupt switching in conductivity in TMD materials by altering the metastable orbital texture. This opens the concept of orbitronics to realize an ultrafast steep switching device based on IMT in 2D materials.

IV. Conclusions

We have shown that the emergence of complex orbital texture intertwined with ligand field stabilization is the underlying mechanism of MIT in 1T″ and monolayer 1T′ phases. We have provided an evidence to modulate the energy band dispersions in a reversible IMT by controlling the orbital texture through external perturbations and an abrupt change in conductance of the order of eight under ballistic limit. This can be a promising insight of future TMD based ultrafast steep slope devices, giving birth to the era of 2D orbitronics.

Acknowledgment

This work was supported by the Center for Low Energy Systems Technology (LEAST), one of six centres of STARnet, a Semiconductor Research Corporation program sponsored by MARCO and DARPA.

References

[1] M. Chhowalla, H. S. Shin, G. Eda, L-J. Li, K. P. Loh, and H. Zhang, "The chemistry of two-dimensional layered transition metal dichalcogenide nanosheet", Nature Chem., vol. 5, pp. 263-275, March 2013.

[2] Y-C. Lin, R. K. Ghosh, R. Addou, N. Lu, S. M. Eichfeld, H. Zhu, M-Y. Li, X. Peng, M. J. Kim, L-J. Li, R. M. Wallace, S. Datta, and J. A. Robinson, "Atomically Thin Resonant Tunnel Diodes built from Synthetic van der Waals Heterostructures", Nature Comm., vol. 6, pp. 7311(1)-(5), June 2015.

[3] R. K. Ghosh, and S. Mahapatra, "Monolayer transition metal dichalcogenide channel based tunnel transistor", IEEE Journal of the Elec. Dev. Soc., vol. 1, pp. 175-180, Nov. 2013.

[4] F. Flicker, and J. van Wezel, "Charge order from orbital-dependent coupling evidenced by $NbSe_2$", Nature Comm., vol. 6, pp. 7034(1)-(6), May 2015.

[5] M. Porer, U. Leierseder, J.-M. Ménard, H. Dachraoui, L. Mouchliadis, I. E. Perakis, U. Heinzmann, J. Demsar, K. Rossnagel, and R. Huber, Nature Mat., vol. 13, pp. 857–861, July 2014.

[6] T. Ritschel, J. Trinckauf, K. Koepernik, B. Büchner, M. v. Zimmermann, H. Berger, Y. I. Joe, P. Abbamonte, and J. Geck, "Orbital textures and charge density waves in transition metal dichalcogenides", Nature Phys., vol. 11, pp. 328–331, March 2015.

[7] QuantumWise Simulator, Atomistix ToolKit (ATK) [Online]. Available: www.quantumwise.com

[8] D. Voiry, A. Mohite, and M. Chhowalla, "Phase engineering of transition metal dichalcogenides", Chem. Soc. Rev., vol. 44, pp. 2702-2712, April 2015.

[9] R. K. Ghosh, M, Brahma, and S Mahapatra, "Germanane: A Low Effective Mass and High Bandgap 2-D Channel Material for Future FETs ", IEEE Trans. Elec. Dev., vol. 61, pp. 2309-2314, July 2014.

[10] F. Tran, and P, Blaha, "Accurate Band Gaps of Semiconductors and Insulators with a Semilocal Exchange-Correlation Potential", Phys. Rev. Lett., vol. 102, pp. 226401(1)-(4), June 2009.